ISSN : 0974 - 746X Volume 7 Issue 1

Trade Science Inc.

Inorganic CHEMISTRY

An Indian Journal

Full Paper

ICAIJ, 7(1), 2012 [9-15]

Synthesis, characterization, thermal behavior and biological activity of some L-histidine metal complexes

Abdullah Sulaiman Al-Ayed

Chemistry Department, Faculty of Science and Arts at El-rass, Qassim University, (KINGDOM OF SAUDI ARABIA)

E-mail: salayedabdualla1@yahoo.com

Received: 9th October, 2011 ; Accepted: 9th November, 2011

ABSTRACT

The L-histidine forming complexes of with Cr(III), Fe(III), Mn(II), Co(II), Ni(II) and Cu(II) of the type 1:1 and 1:2 (M:L) have been synthesized and characterized by means of elemental analysis, molar conductance, IR spectra, thermal analysis, UV-Vis spectra, magnetic moment and ESR spectra. The low molar conductance values suggest the non-electrolytic nature of these complexes. Spectroscopic and other analytical studies revealed a square planar geometry for copper complexes and octahedral geometry for the other complexes. The thermal behavior of these complexes indicated that the hydrated complexes loss water of hydration in first step followed by the loss of coordinated water and chloride immediately. The activation thermodynamic parameters, such as ΔE^*, ΔH^*, ΔS^*, and ΔG^* are calculated using Coats–Redfern method. Antimicrobial activity of L-histidine and its complexes has been tested against different microorganisms.

KEYWORDS

L-histidine;
Metal complexes;
Spectral studies;
Thermal behavior;
Biological activity.

INTRODUCTION

The presence of L-histidine has been established in a large number of the active centers of enzymes[1] and the histidyl residue is probably the most important metal-binding site in biological systems[2-5]. L-histidine has four expected binding sites; carboxylate-O, amine-N and two imidazole-Ns. The heterocyclic imidazole ring system in the histidine side chain provides bidentate ligand with two competitive N3 and N1 donor atoms. The metal complexes of L-histidine have been investigated[6-9]. In most metal complexes with histidine-containing ligands, the imidazole ring of histidine is coordinated through the N3 nitrogen[10-12] but relatively few complexes in which histidine is coordinated only through the N1 atom have been well characterized[13]. There are also some reports about the coordination of L-histidine to the metal center through carboxylate-O and amine-N[14,15].

The aim of the present study is to synthesize Cr(III), Fe(III), Mn(II), Co(II), Ni(II), and Cu(II) complexes of L-histidine, which acts as bidentate ligand, reacted with the metal salts in the molar ratio 1:1(M:L) and 1:2 (M:L) resulting in the formation of complexes. The prepared complexes were characterized by different methods of analysis. The L-histidine and its metal complexes display obvious inhibitor effect against gram positive bacteria (Staphylococcus aures and Bacillus subtilis) and gram negative bacteria (Escherichia coli and pesudo monos aerogenas). These studies reported the minimum inhibitor concentration of the used Schiff base and its metal complexes on these microorganism[16].

EXPERIMENTAL

Synthesis of the metal complexes

To a solution of histidine in 1:1methanol:water (20 ml) was added a solution of metal chloride (1 mmol) in methanol in the molar ratio 1:1 or 2:1, respectively. The resulting solutions were then refluxed in a water bath for 4 hours. The solid complexes, which separated out on hot, were filtered off, washed several times with ether and finally dried under vacuum.

Physical measurements

Elemental analyses were performed by the aid of Heraeus CHN analyzer. IR spectra were recorded on a Perkin Elmer 1430 instrument (KBr discs) in the range 4000-200 cm^{-1}. Electronic spectra were obtained with a Shimadzu UV-Vis. 240 spectrophotometer by using nujol mull technique. The ESR spectra of powder samples were recorded by means of a Jeol model JES-FE 2XG spectrometer equipped with an E101 microwave bridge. Diphenyl picrylhydrazyl (DPPH) was used as a reference material ($g = 2.0023$). The molar conductance measurements were carried out at room temperature using Hanna 8733 conductivity meter. The room temperature magnetic susceptibility was measured using magnetic susceptibility balance (Johnson Mtthey) 436 Devon Park Drive. The thermal analyses (TGA and DTG) were performed using computerized Shimadzu TG-50 thermal analyzer up to 800 °C at a heating rate 10 °C/min under nitrogen atmosphere.

The nutrient agar solid medium contained per 1000 ml (pH=7.2): beef extract 3gm, peptone 5gm, Nail 5gm and agar 20gm. It was sterilized in high pressure steam for 30 min., serial dilutions of the and L-histidine its complexes were prepared containing 250 μg/ml down to 3 μg/ml. The bacteria used for testing the biological activity of the ligand and their complexes were Gram positive bacteria (Staphylococcus aures and Bacillus subtilis) and Gram negative bacteria (Escherichia coli and pesudomonos auerogenas) provided by the biology department. It was found that these bacteria exhibit obvious sensitivity towards organic and organic metal complexes.

RESULTS AND DISCUSSION

Elemental analysis and molar conductance

Elemental analysis of the prepared metal complexes (TABLE 1) indicate that the stoichiometric ratio are (1:1 and 1:2) (M:L), in which the ligand behaves as monoanionic bidentate indicating the formation of complexes. The molar conductance values, as 10^{-4} M solutions in DMF at 25°C, indicate that all the metal complexes are non-electrolytic in nature[17].

IR spectra

The important IR frequencies of L-histidine and its complexes are given in TABLE 2. The band corresponding to ν_{COO} band of L-histidine shows a shift towards lower wavenumber in the spectra of metal complexes providing evidence that L-histidine is bonded to the metal ion through the carboxylic group[18]. The two bands which appear at 3374 and 3160 cm^{-1} in the spectra of L-histidine are due to $\nu_{asym}(NH_2)$ and $\nu_{sym}(NH_2)$ vibrations of the NH_2 group[19]. These vibration modes appear at lower wavenumbers in the spectra of metal complexes indicating the coordination of the amino group to the metal center. The two bands corresponding to C-N and C=N groups of imidazole moiety which appeared in the ligand spectra at 1520 and 1470 cm^{-1}, do not shift in the spectra of metal complexes suggesting non-involvement of imidazole moiety in coordination. The appearance of bands in the range 3459–3421 cm^{-1} and 790–828 cm^{-1} is due to the stretching vibration and out of plane bending of coordinated water molecules in the spectra of the metal complexes. The non-ligand bands appearing in the region 567-505 and 482-418 cm^{-1} confirm the coordination of oxygen and nitrogen atoms to the metal centers.

Magnetic moment and electronic spectra

The Cr(III) complexes 1 and 7 of the type M:L (1:1 and 1:2) show μ_{eff} values of 3.99 and 3.89 B.M, respectively, corresponding to three unpaired electrons indicating an octahedral geometry around the Cr center. The two complexes are expected to show three spin allowed d-d transitions that are ${}^4A_{2g}(F) \rightarrow {}^4T_{2g}(\nu_1)$,

TABLE 1 : Analytical and electronic spectral data of the prepared compounds.

Comp. No.	Formula	colour	L:M ratio	m.p. (°C)	Λ^a	Analysis Found (calcd.) % %C	%H	%N	$_{\text{eff}}\mu$	λ_{max} (nm)
1	$[Cr(L)(H_2O)_2Cl_2]$	Deep green	1:1	>300	15.6	23.51 (23.0)	3.43 (3.83)	13.9 (13.42)	3.99	538, 336
2	$[Fe(L)Cl_2(H_2O)_2]$	Brown	1:1	>300	17.4	22.23 (22.73)	3.42 (3.79)	13.87 (13.26)	5.65	488, 410
3	$[Mn(L)(H_2O)_3Cl]$	Brown	1:1	270	10.5	24.94 (24.12)	4.32 (4.69)	14.87 (14.07)	5.54	698, 482, 406
4	$[Ni(L)(H_2O)_3Cl]H_2O$	Green	1:1	290	11.3	23.76 (23.83)	4.82 (4.63)	13.32 (13.90)	3.32	679, 559, 456
5	$[Co(L)(H_2O)_3Cl]H_2O$	Faint brown	1:1	288	10.4	21.96 (22.47)	5.41 (4.99)	12.96 (13.11)	4.78	546, 432
6	$[Cu(L)(H_2O)Cl]2H_2O$	Dark green	1:1	>300	12.5	23.16 (23.45)	4.99 (4.56)	13.94 (13.68)	1.83	490
7	$[Cr(L)_2(H_2O)Cl]$	Green	2:1	289	12.4	34.29 (34.82)	4.96 (4.35)	20.75 (20.31)	3.89	531,345
8	$[Fe(L)_2(H_2O)Cl]2H_2O$	Deep brown	2:1	>300	14.6	31.23 (31.76)	4.28 (4.85)	18.20 (18.53)	5.74	493, 399
9	$[Mn(L)_2(H_2O)_2]H_2O$	Brown	2:1	299	8.5	34.27 (34.54)	5.11 (5.28)	20.58 (20.15)	5.87	680, 490, 399
10	$[Ni(L)_2(H_2O)_2]2H_2O$	Green	2:1	>300	7.6	32.04 (32.82)	5.29 (5.47)	19.84 (19.15)	3.12	687, 547, 451
11	$[Co(L)_2(H_2O)_2]$	Faint brown	2:1	278	8.9	35.98 (35.74)	4.54 (4.96)	20.58 (20.85)	4.86	532, 429
12	$[Cu(L)_2]2H_2O$	Dark green	2:1	>300	9.5	35.04 (35.34)	5.19 (4.91)	20.97 (20.61)	1.81	495

^{a} Ω^{-1} cm^2 mol^{-1}

TABLE 2 : Important IR spectral bands and their assignments of ligands and their metal complexes.

Compound	υ_{OH}	υ_{NH2}(asy)	υ_{NH2}(sym)	υ_{Coo}	υ_{C-N}	$\upsilon_{C=N}$	υ_{M-O}	υ_{M-N}
L-histidine	-	3374	3160	1575	1522	1471	-	-
1	3420	3348	3130	1553	1523	1469	567	423
2	3441	3343	3100	1546	1522	1470	534	476
3	3459	3353	3147	1555	1521	1473	556	467
4	3427	3350	3142	1543	1522	1472	545	445
5	3421	3352	3129	1544	1523	1468	560	463
6	3451	3346	3139	1555	1522	1471	550	435
7	3433	3349	3145	1552	1521	1472	560	421
8	3434	3350	3149	1556	1520	1470	545	482
9	3445	3353	3147	1553	1522	1470	563	418
9	3444	3348	3144	1549	1521	1472	545	473
10	3456	3349	3145	1556	1522	1470	540	446
11	3424	3351	3133	1556	1520	1473	537	429
12	3440	3345	3140	1553	1520	1471	505	439

$^4A_{2g}(F) \rightarrow {}^4T_{1g}(\nu_2)$ and $^4A_{2g}(F) \rightarrow {}^4T_{1g}$ (P)[20]. The two complexes 1 and 7, show two bands at 538, 531 nm (ν_1) and 336, 345 nm (ν_2), respectively. The third band expected to appear below 300 nm and overlapped with L → M charge transfer band.

The observed magnetic moment values Fe(III) complexes of the type M:L (1:1 and 1:2) were found to be 5.65 and 5.74 B.M is consistent with an octahedral geometry. The electronic spectra of these two complexes show two bands at 488, 410 nm for complex 2 and 493, 399 nm for complex 8 which can be assigned to $^6A_{1g} \rightarrow {}^4T_{1g}$ and $^6A_{1g} \rightarrow {}^4T_{2g}$ transitions characteristic for octahedral geometry around the Fe center[13].

For the Mn(II) complexes of the type M:L (1:1 and 1:2), the magnetic moment values are found to be 5.54 and 5.87 B.M for complexes 3 and 8, respectively, which indicates octahedral geometry around the Mn(II) ion[21]. The electronic spectrum of the Mn(II) complex shows three bands at 698, 482 and 406 nm for complex 3 and 680, 490 and 399 nm for complex 8 which are assigned to $^4A_{1g} \rightarrow {}^6A_{1g}$, $^4T_{2g}(G) \rightarrow {}^6A_{1g}$ and $^4T_{1g}(D) \rightarrow {}^6A_{1g}$ transitions, respectively, confirming the octahedral geometry around the metal center.

The magnetic moment values of the Ni(II) complexes 4 and 10 of the type M:L (1:1 and 1:2) are found to be 3.32 and 3.12 B.M. for complexes 4 and 10, respectively, which falls within the range normally observed for octahedral Ni(II) complexes[21]. The electronic spectra of the Ni(II) complexes show recognizable spectral bands at 679, 559 and 456 nm for complex 4 and at 687, 547 and 451 nm for complex 10 which assigned to $^3A_{2g} \rightarrow {}^3T_{2g}$, $^3A_{2g} \rightarrow {}^3T_{1g}$ (F) and

$^3A_{2g} \rightarrow {}^3T_{1g}$ (P) transitions, respectively.

The magnetic moment values of the Co(II) complexes 5 and 11 of the type M:L (1:1 and 1:2) are found to be 4.78 and 4.86 B.M. which are consistent with high-spin octahedral cobalt(II) complexes. The electronic spectra of the complexes in DMF confirmed their octahedral stereochemistry. The electronic spectra of both complexes show two bands at 546 and 432 nm for complex 5 and at 532 and 429 nm for complex 11, which may be assigned to $^4T_{1g}(F) \rightarrow {}^4T_{2g}$ and $^4T_{1g}(F) \rightarrow {}^4T_1(P)$ transitions, respectively, of pseudo-octahedral cobalt(II) complexes[23].

The magnetic moment values of the Cu(II) complexes 6 and 12 of the type M:L (1:1 and 1:2) are 1.83 and 1.81 BM corresponding to one unpaired electron. The former complex shows a band at 490 nm while the later complex show a band at 495 nm due to $^2B_{1g} \rightarrow {}^2E_g$ suggesting square planar structure of Cu(II) complexes[20].

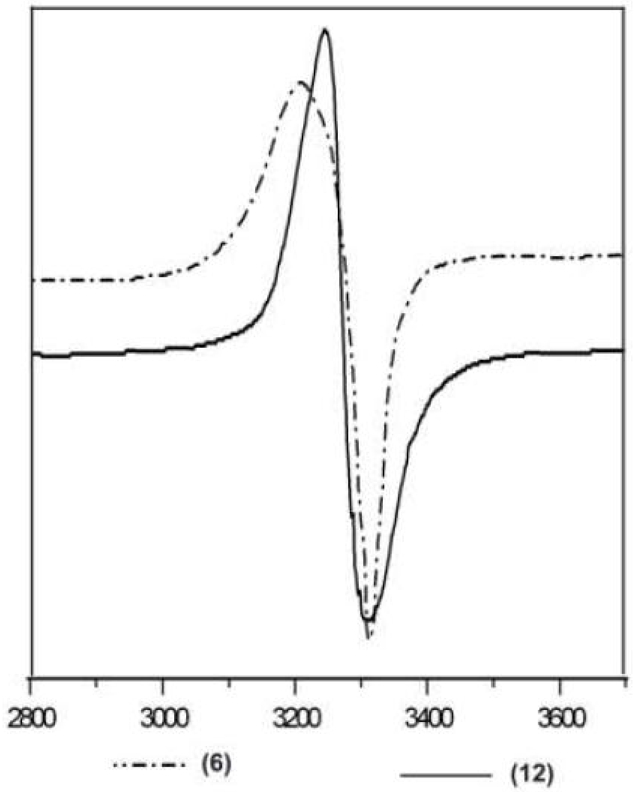

Figure 1 : X-band ESR spectra of Cu(II) complexes 6 and 12 measured at room temperature

Thermal analysis

The TG curves of Mn(II) complex 3 and Cu(II) complex 12 give three-stage decomposition pattern within the range 100-546 and 30-530 °C, respectively. The first step corresponds to the loss of coordinated and lattice water within the ranges 100-220 and 30-110 °C, respectively. The second step for complex 3 occurs within the temperature range 220-300 °C and involve the loss of HCl. The organic ligands decompose in the second and third decomposition steps within the temperature range 300-546 °C for complex 3 and within the ranges 216-310 and 310-530 °C for complex 12 resulting in the formation of MnO and CuO, respectively, as final products.

The TG curves of Cr(III) complex 1 and Ni(II) complex 10 give pattern four successive decomposition steps within the ranges 90-590 and 28-515 °C, respectively. The first step attributed to the loss of coordinated and lattice water within the temperature ranges 90-180 and 28-117 °C for complex 1 and 10, respectively. The second step occurs within the temperature range 180-290 °C for complex 1 and 117-220 °C for complex 10, and involve the loss HCl and coordinated water, respectively. The third step involves the decomposition of the organic ligand with elimination of imidazole moiety and occurs in the within the temperature ranges 290-450 and 220-320 °C for complexes 1 and 10, respectively. The two complexes are further decomposed within the temperature range 450-590 and 320-515 °C for complexes 1 and 10 with the formation of Cr_2O_3 and NiO, respectively, as final products.

The Co(II) complex 5 and Fe(III) complex 8 decompose in five successive decomposition steps. The first two steps are assigned to the loss of lattice and coordinated water and appear within the range 28-160 and 28-190 °C for complexes 5 and 8, respectively. The third step occur within the temperature ranges 160-234 and 190-276 °C for complexes 5 and 8, respectively, and involve the loss of HCl. The organic ligands decompose in two successive steps within the temperature ranges 234-650 and 276-622 °C leaving behind CoO and Fe_2O_3 as product of decomposition for complexes 5 and 8, respectively.

Kinetic studies

According to the kinetic data obtained from TG and DTG curves, the thermodynamic activation parameters of the various decomposition steps of the metal complexes (ΔE*, ΔH*, ΔS* and ΔG*) were evaluated graphically by employing the Coats–-Redfern relations[24]. The data obtained are summarized in TABLE 4. The data obtained also show that the activation energies of decomposition are found to be in the range 16.79–284.84 kJ/ mol. The high values of the activation energies reflect the thermal stability of the metal complexes. The entropy of activation is found to be negative for all the metal complexes, which indicate that the decomposition reactions proceed with a lower rate than the normal ones[25,26] and/ or the activated complexes have more ordered systems than reactants.

TABLE 3 : Thermogravimetric data of some selected metal complexes.

Comp. No.	Complex (molecular weight)	TG range (C)	DTG temp. (C)	(Calc.)found mass loss %	Assignment
1	$[Cr(L)(H_2O)_2Cl_2]$ $C_7H_{15}N_3Cl_2O_4Cr$ (328.11)	90-180	130	(10.97) 10.55	- Loss of coordinated H_2O
		180-290	235	(21.94)21.65	- Loss of 2HCl
		290-450	362	(20.44) 20.02	- Loss of imidazole part
		450-590	460	(21.63) 22.31	- Further decomposition of ligand and formation of $0.5Cr_2O_3$ as final product
3	$[Mn(L)(H_2O)_3Cl]$ $C_7H_{17}N_3ClO_5Mn$ (313.62)	100-220	150	(17.21) 18.11	- Loss of coordinated H_2O
		220-300	240	(11.63) 12.32	- Loss of HCl
		300-546	494	(44.12) 44.87	- decomposition of ligand and formation of MnO as final product
5	$[Co(L)(H_2O)_3Cl]H_2O$ $C_7H_{19}N_3ClO_6Co$ (335.63)	28-90	70	(5.36) 5.96	- Loss of lattice H_2O
		90-160	144	(16.08)16.78	- Loss of coordinated H_2O
		160-234	221	(10.87) 10.63	- Loss of HCl
		234-400	340	(19.98) 19.32	- Loss of imidazole part
		400-650	580	(21.15) 21.68	- Further decomposition of ligand and formation of CoO as final product
8	$[Fe(L)_2(H_2O)Cl]2H_2O$ $C_{13}H_{25}N_6ClO_7Fe$ 468.08	28-110	65	(7.69) 7.45	- Loss of lattice H_2O
		110-190	160	(3.84)4.32	- Loss of coordinated H_2O
		190-276	243	(7.81) 7.98	- Loss of HCl
		276-430	330	(28.62) 28.98	- Loss of imidazole part
		430-622	530	(30.33) 30.87	- Further decomposition of ligand and formation of $0.5Fe_2O_3$ as final product
10	$[Ni(L)_2(H_2O)_2]2H_2O$ $C_{13}H_{27}N_6O_8Ni$ (454.08)	28-117	75	(7.92) 7.15	- Loss of lattice H_2O
		117-220	170	(7.92)7.63	- Loss of coordinated H_2O
		220-320	293	(7.81) 7.98	- Loss of imidazole part
		320-515	440	(31.30) 31.98	- Further decomposition of ligand and formation of NiO as final product
12	$[Cu(L)_2]2H_2O$ $C_{13}H_{23}N_6O_6Cu$ 422.90	30-110	66	(8.51) 9.75	- Loss of lattice H_2O
		216-310	250	(31.71)31.23	- Loss of imidazole part
		310-530	465	(33.57) 33.48	- Further decomposition of ligand and formation of CuO as final product

TABLE 4 : Thermodynamic data of the thermal decomposition of the metal complexes.

Compound	Step	TG range (°C)	E* (kJ/mol)	A (kJ/mol)	ΔS* (kJ/K mol)	ΔH* (kJ/mol)	ΔG* (kJ/mol)
1	1st	90-180	56.72	4.17×10^8	-33.16	35.25	55.02
	2nd	180-290	92.17	2.54×10^6	-72.82	66.75	76.22
	3rd	290-450	81.93	1.41×10^4	-0.18	76.41	196.2
	4th	450-590	280.1	1.54×10^{19}	0.11	274.4	201.1
3	1st	100-220	54.71	6.4×10^6	-0.12	52.00	92.11
	2nd	220-300	24.19	2.03×10^5	-0.15	20.36	95.62
	3rd	300-546	41.50	3.331	-0.24	36.26	193.1

Compound	Step	TG range (°C)	E* (kJ/mol)	A (kJ/mol)	ΔS* (kJ/K mol)	ΔH* (kJ/mol)	ΔG* (kJ/mol)
5	1st	28-90	53.86	4.33×10^{4}	-0.16	50.90	109.8
	2nd	90-160	11.68	0.019	-0.29	8.161	132.4
	3rd	160-234	81.93	1.41×10^{4}	-0.18	76.41	196.2
	4th	234-400	280.1	1.54×10^{19}	0.11	274.4	201.1
	5th	400-650	176.9	1.60×10^{10}	-0.06	170.8	218.3
8	1st	28-90	45.293	23.1×10^{3}	-0.171	42.371	102.47
	2nd	90-160	53.198	18.4×10^{3}	-0.174	49.778	121.45
	3rd	160-234	82.562	1.123×10^{6}	-0.142	78.387	149.56
	4th	234-400	93.255	142.4×10^{3}	-0.161	88.043	188.84
	5th	400-650	15.918	1.799×10^{-3}	-0.315	7.884	312.83
10	1st	28-117	83.35	1.26×10^{10}	-0.06	80.65	100.3
	2nd	117-220	57.38	1.37×10^{5}	-0.15	53.86	120.7
	3rd	220-320	28.41	0.221	-0.27	23.24	191.8
	4th	320-515	130.2	6.3×10^{6}	-0.13	124.2	217.5
12	1st	30-110	251.5	2.33×10^{32}	0.31	248.3	130.6
	2nd	216-310	34.52	2.859	-0.24	29.92	162.8
	3rd	310-530	106.9	8.16×10^{6}	-0.12	101.7	180.1

ESR spectra

The ESR spectrum of Cu(II) complexes 6 and 12, in the solid state, was measured at room temperature. The calculated data show that g_{11} = 2.21 & 2.28 and $g_{\perp}$ = 2.09 & 2.06 for complexes 6 and 12, respectively i.e. $g_{11} > g_{\perp} > 2.0023$. This indicates that the unpaired electron is localized in d_{x2-y2} orbital[26], which is consistent with the proposed planar stereochemistry[28]. Also, the observed value which is <2.3 indicates the covalent nature between the Cu(II) ion and the ligand[29].

The structures of the complexes are given in Schemes 1 and 2.

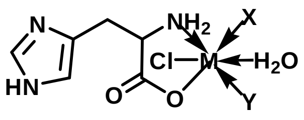

1	M= Cr(III)	X=Cl	Y=H_2O
2	M=Fe(III)	X=Cl	Y=H_2O
3	M=Mn(II)	X=Y= H2O	
4	M=Ni(II)	X=Y= H_2O	
5	M=Co(II)	X=Y= H_2O	
6	M=Cu(II)	X=Y=0	

Scheme 1

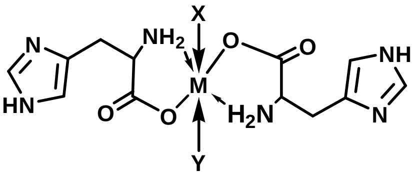

7	M= Cr(III)	X=Cl	Y=H_2O
8	M=Fe(III)	X=Cl	Y=H_2O
9	M=Mn(II)	X=Y= H2O	
10	M=Ni(II)	X=Y= H_2O	
11	M=Co(II)	X=Y= H_2O	
12	M=Cu(II)	X=Y=0	

Scheme 2

Biological activity

A primary study of the Minimum inhibitor concentrations (MIC) of L-histidine and its complexes on Gram positive bacteria (Staphylococcus aures and Bacillus subtilis) and Gram negative bacteria (Escherichia coli and pesudo monos aerogenas) are recorded in (TABLE 5).

From (TABLE 5) it is clear that the inhibition is much larger for metal complexes than that of L-histidine on gram positive and gram negative bacteria. The Cu(II) complexes (6 and 12) have the most inhibitor effect on gram negative and gram positive bacteria than the other metal complexes. The antibiotic effect of bi-ligand Cu(II) complex (12) on Gram negative and Gram positive bacteria is relatively stronger than complex (6). AS gathered from the data given in TABLE 5, the order of inhibition of all complexes in the activity of the bacteria studied can be arranged as follows: For Escherichia coli the complex 12< 6< 4< 9< 3,11< 2

<ligand, for Pesudomonos aeruginosa the complex 12< 6< 9,11< 2 <4< 3 <ligand, for Bacillus subtilis the complex 12 < 6< 11< 4< 2< 9< 3< ligand and for Staphylococcus aureus the complex 12 <4< 6 < 9 <3< 2,11 < ligand. Such increased activity of the metal chelates can be explained on the basis of chelation theory[30]. On chelating, the polarity of the metal ion will be reduced to a great extent due to the overlap with the ligand orbital. Further, it increases the delocalization of π-electrons over the whole chelae ring and enhances the lipophilicity of the complexes[31].

TABLE 5 : Minimum inhibitor concentration of L-histidine and complexes against gram +ve and gram -ve bacteria.

Organism	Gram -ve bacteria		Gram +ve bacteria	
Compound	**E-Coli**	**Ps-aur**	**B-sub**	**St-aur**
L-histidine	150	150	100	250
Complex 2	100	60	50	100
Complex 3	50	90	100	85
Complex 4	35	80	6.8	25
Complex 6	5.1	40	4.5	30
Complex 9	40	50	80	45
Complex 11	50	50	5.7	100
Complex 12	3.1	35	3.5	15

REFERENCES

[1] F.Schneider; Angew.Chem.Int.Ed.Engl., **17**, 583 **(1978)**.

[2] R.J.Sundberg, R.B.Martin; Chem.Rev., **74**, 471-517 **(1974)**.

[3] A.S.Brill; Transition Metals in Biochemistry, Springer-Verlag, New York, Chapt. 2, **(1977)**.

[4] D.Rehder; Inorg.Chem.Commun., **6**, 604 **(2003)**.

[5] M.R.Maurya, S.Agarwal, C.Bader, D.Rehder; Eur. J.Inorg.Chem., **147**, **(2005)**.

[6] H.Yue, D.Zhang, Y.Chen, Z.Shi, S.Feng; J.Inorg. Commun., **9**, 959 **(2006)**.

[7] P.Kaczmarek, M.J.Bojezuk, W.Bal, K.S.Kasprzak; J.Inorg.Biochem., **99**, 737 **(2005)**.

[8] M.J.Bojezuk, P.Kaczmarek, W.Bal, K.S.Kasprzak; J.Inorg.Biochem., **98**, 1770 **(2004)**.

[9] P.Drevensek, T.Zupancic, B.Pihlar, R.Jerala, U.Kolitsch, A.Plaper, I.Turel; J.Inorg.Biochem., **99**, 422 **(2005)**.

[10] K.A.Fraser, M.M.Harding; J.Chem.Soc.A, 415-420 **(1967)**.

[11] I.A.Baidina, O.P.Slyudkin, S.V.Borisov; Zh.Strukt. Khim., **26**, 139-142 **(1985)**.

[12] B.Evertsson, C.Lundgren; Acta Chem.Scand., **20**, 2310-2311 **(1966)**.

[13] K.Krogh-Jespersen, J.D.Westbrook, J.A.Potenza, H.J.Schugar; J.Am.Chem.Soc., **109**, 7025-7031 **(1987)**.

[14] K.Narang, V.Singh, D.Bhattacharya; Polyhedron., **16**, 2491 **(1996)**.

[15] H.Yue, D.Zhang, Y.Chen, Z.Shi, S.Feng; Inorg.Chem. Commun., **9**, 959 **(2006)**.

[16] C.Jayabalakrishnan, K.Natarajan; Transition Met. Chemistry, **27**, 75 **(2002)**.

[17] W.J.Geary; Coord.Chem.Rev., **7**, 81 **(1971)**.

[18] L.Larson; Acta Chem.Scand., **4**, 27 **(1950)**.

[19] A.G.Raso, J.J.Fiol, S.Rigo, A.L.Lopez, E.Molins, E.Espinosa, E.Borras, G.Alzuet, J.Borras, A.Castineiras; Polyhedron., **19**, 991 **(2000)**.

[20] A.B.P.Lever; Inorganic Electronic Spectroscopy, Second Edition, Elsevier, Amsterdam, **(1984)**.

[21] F.A.Cotton, G.Wilkinson, C.A.Murillo, M.Bochmann; Advanced Inorganic Chemistry, 6th Edition, Wiley, New York, **(1999)**.

[22] C.M.Sharaby; Spectrochimica Acta, Part A, **66**, 1271 **(2007)**.

[23] C.M.Sharaby; Spectrochimica Acta, Part A, **62**, 326 **(2005)**.

[24] A.W.Coats, J.P.Redfern; Nature, **201**, 68 **(1961)**.

[25] A.I.El-Said, A.A.Aly, A.S.Zidan; J.Therm.Anala., **37**, 2473 **(1991)**.

[26] A.A.Frost, R.G.Pearson; Kinetics and Mechanism, John Wiley and Sons, New York, **(1961)**.

[27] R.C.Agarwal, N.K.Singh, R.P.Singh; Inorg.Chem., **20**, 2794 **(1981)**.

[28] D.N.Kumar, B.K.Singh, B.S.Garg, P.K.Singh; Spectrochim.Acta A, **59**, 1487 **(2003)**.

[29] D.Kivelson, R.Neiman; J.Chem.Phys., **35**, 149 **(1961)**.

[30] R.S.Srivastava; Inorg.Chim.Acta, **56**, 65 **(1981)**.

[31] N.Gupta, R.Swaroop, R.V.Singh; Main Group Met. Chem., **14**, 387 **(1997)**.